

Quadruple bonds in MoC: Accurate calculations and precise measurement of the dissociation energy of low-lying states of MoC

Alexandros Androustopoulos,^[a] Demeter Tzeli,^{[a,b],*}

Kimberly H. Tomchak,^[c] and Michael D. Morse^{[c],*}

^[a] Laboratory of Physical Chemistry, Department of Chemistry, National and Kapodistrian University of Athens, Panepistimiopolis Zografou, Athens 157 84, Greece

^[b] Theoretical and Physical Chemistry Institute, National Hellenic Research Foundation, 48 Vassileos Constantinou Ave., Athens 116 35, Greece

^[c] Department of Chemistry, University of Utah, Salt Lake City, Utah 84112, USA

* Corresponding Authors: tzeli@chem.uoa.gr, morse@chem.utah.edu

Tel: +30-210-727-4307, +1-801-581-8319

ABSTRACT

In the present work, the electronic structure and chemical bonding of the MoC $X^3\Sigma^-$ ground state, and of the six lowest excited states, $A^3\Delta$, $a^1\Gamma$, $b^5\Sigma^-$, $c^1\Delta$, $d^1\Sigma^+$, and $e^5\Pi$, have been investigated in detail using multireference configuration interaction methods and basis sets including relativistic effective core potentials. Additionally, scalar relativistic effects have been considered in the second order Douglas–Kroll–Hess approximation, while spin-orbit coupling has also been calculated. Five of the investigated states, $X^3\Sigma^-$, $A^3\Delta$, $a^1\Gamma$, $c^1\Delta$, and $d^1\Sigma^+$, present quadruple $\sigma^2\sigma^2\pi^2\pi^2$ bonds. Experimentally, the predissociation threshold of MoC was measured using resonant two-photon ionization spectroscopy, allowing for a precise measurement of the dissociation energy of the ground state. Theoretically, the complete basis set limit of the calculated dissociation energy, with respect to the atomic ground state products, including corrections for scalar relativistic effects, $D_e(D_0)$, is computed as 5.13(5.06) eV, in excellent agreement with our measured value of $D_0(\text{MoC})$ of 5.136(5) eV. Furthermore, the calculated dissociation energies of the states having quadruple bonds with respect to their adiabatic atomic products range from 6.22 eV to 7.23 eV. The excited electronic states $A^3\Delta_2$ and $c^1\Delta_2$ are calculated to lie at 3899 cm^{-1} and 8057 cm^{-1} , also in excellent agreement with the experimental values of DaBell *et al.*, 4002.5 and 7834 cm^{-1} , respectively.

This is the author's peer reviewed, accepted manuscript. However, the online version of record will be different from this version once it has been copyedited and typeset.
PLEASE CITE THIS ARTICLE AS DOI: 10.1063/5.0211422

ACCEPTED MANUSCRIPT

The Journal of
Chemical Physics

AIP
Publishing

11 February 2025 09:27:56

I. INTRODUCTION

Transition metal compounds have a wide range of applications, since they play a key role in such diverse areas as organometallic chemistry, catalysis, surface science, and astrophysics [1]. Their theoretical calculation can be quite complex due to the high density of states and the high spin and orbital angular momentum of the constituent transition metal atom.[2] The investigation of diatomic molecules that contain transition metals can provide valuable insights into the properties of more complex transition metal systems.

Transition metal–carbon bonds, and specifically the molybdenum-carbon bond, are involved in many fields such as homogeneous and heterogeneous catalysis, organometallic chemistry, biology, high temperature chemistry, materials science, *etc.*[3-4] As a result, the study of diatomic MoC has attracted both theoretical and experimental attention. In total, nine studies of diatomic MoC have been published, as summarized in Table 1. In 1981, Gupta and Gingerich [5] performed a Knudsen effusion mass spectroscopic study of the reaction $\text{Mo(g)} + \text{C(graphite)} \rightleftharpoons \text{MoC(g)}$. From the measured equilibrium constant and the literature value of the vaporization enthalpy of graphite, the bond dissociation energy (BDE) of MoC was determined to be $D_0 = 4.95 \pm 0.17$ eV. In 1997, Shim and Gingerich [6] carried out a series of all electron *ab initio* CASSCF and MRCI calculations that included relativistic corrections so as to determine the molecule's low-lying electronic states. As for the ground state, $X_{\square}^3\Sigma^-$, the obtained results are $r_e = 1.693$ Å, $\omega_e = 971$ cm⁻¹ and $D_e = 5.20$ eV. In 1998, Brugh *et al.* performed the first optical spectroscopic investigation of MoC [7]. It was deduced that the ground state is the $\Omega = 0^+$ spin–orbit component of a $\square^3\Sigma^-$ state with $r_0 = 1.6760$ Å. In 1999, Li *et al.* measured the electron affinity of MoC using photoelectron spectroscopy and identified several excited electronic states.[8] In 2001, Morse *et al.* performed a dispersed fluorescence study of MoC [9]. In that work, the term energies and vibrational frequencies of the $\square^3\Delta_2$ and $\square^1\Delta_2$ states were measured. It was found that the $\square^3\Delta_2$ state lies at 4002.5 cm⁻¹ while the $\square^1\Delta_2$ state lies at 7834 cm⁻¹. In 2006, Denis and Balasubramanian [10] investigated the potential energy curves and spectroscopic constants of the ground and 29 low-lying excited states of MoC with various spin and orbital angular momentum symmetries within 48000 cm⁻¹ by employing the CASSCF methodology, followed by MRCI methods. In the same year, Stevens *et al.* [11] calculated the equilibrium bond length, dipole moment, and harmonic vibrational frequency of the ground $X_{\square}^3\Sigma^-$ state of MoC using flexible basis sets comprised of Slater type functions and a series of exchange correlation functionals. The results obtained using the BP86 functional form are $r_e = 1.667$ Å, $\mu = 5.209$ D and $\omega_e = 1034.7$ cm⁻¹. In 2007, the Steimle group employed high-resolution Stark spectroscopy to measure the dipole moment of MoC in the $v=0$ levels of the $X_{\square}^3\Sigma^-$ ground and $[18.6]^3\Pi_1$ states.[12] In 2015, Liu

This is the author's peer reviewed, accepted manuscript. However, the online version of record will be different from this version once it has been copyedited and typeset. PLEASE DO NOT DISTRIBUTE OR IDENTIFY THIS ARTICLE BEFORE THE FINAL PUBLISHED VERSION. DOI: 10.1063/1.5014242

et al [13] studied the isoelectronic diatomic MoC⁻ and NbN⁻ anions via photoelectron imaging spectroscopy combined with quantum chemistry calculations. Within this context, a series of *ab initio* calculations were carried out to investigate the ground state structures and energies of the MoC⁻ and NbN⁻ ions and their neutral counterparts. At the CCSD(T)/aug-cc-pwCVQZ(-PP) computational level, the MoC ground state equilibrium distance, r_e , is 1.660 Å.

The aim of the present work is the accurate investigation of the electronic structure and the chemical bonding of the lowest energy states, with a view to clarifying their bonding patterns as well as determining the ground state dissociation energy. Spectroscopic data and potential energy curves of these seven states, $X^3\Sigma^-$, $A^3\Delta$, $a^1\Gamma$, $b^5\Sigma^-$, $c^1\Delta$, $d^1\Sigma^+$, and $e^5\Pi$, employing multireference configuration interaction methodologies along with a series of basis sets have been obtained. Additionally, relativistic effects and spin-orbit interactions are considered. Furthermore, the bond dissociation energy of the ground state is precisely measured using resonant two-photon ionization (R2PI) spectroscopy. Finally, the five low-lying states, $X^3\Sigma^-$, $A^3\Delta$, $a^1\Gamma$, $c^1\Delta$ and $d^1\Sigma^+$, which all correlate to excited separated atom limits, are found to form quadruple bonds. This is uncommon in diatomic molecules containing second row atoms. [14, 15] The $b^5\Sigma^-$ and $e^5\Pi$ states, which correlate to ground state separated atom limits, form two and a half bonds.

II. COMPUTATIONAL METHODOLOGY

The $X^3\Sigma^-$, $A^3\Delta$, $a^1\Gamma$, $b^5\Sigma^-$, $c^1\Delta$, $d^1\Sigma^+$, and $e^5\Pi$ states were calculated via multireference methodology. A series of basis sets were used in order to: (i) evaluate the importance of core electrons, (ii) compare and check the results obtained using basis sets including relativistic pseudopotentials and using full electron Douglas-Kroll consistent basis sets, and (iii) calculate Complete Basis Set (CBS) limits for the main spectroscopic data. Thus, both augmented correlation consistent basis sets for valence electrons and augmented weighted core correlation consistent basis sets were used, *i.e.*, aug-cc-pV5Z(-PP) and aug-cc-pwCV5Z(-PP). [16-18]. Furthermore, the CBS limits of the main spectroscopic data were calculated via the series of aug-cc-pwCV n Z, $n = D(2)$, T(3), Q(4), and 5 basis sets. Finally, relativistic effects, *i.e.*, mass-velocity and Darwin terms, are considered by the second order Douglas-Kroll-Hess (DKH2) approximation, [19] employing full electron Douglas-Kroll consistent basis sets, *i.e.*, aug-cc-pwCVTZ-DK and aug-cc-pVTZ-DK. In detail, for the Mo atom, the largest used basis set including relativistic pseudopotentials is the aug-cc-pwCV5Z-PP which is contracted to [10s10p9d6f5g4h3i], while the largest full electron Douglas-Kroll consistent basis set is the aug-cc-pwCVTZ-DK contracted to [11s10p8d4f3g]. For the C atom, the largest basis set is the aug-cc-pwCV5Z contracted to [11s10p8d6f4g2h].

At first, the complete active space self-consistent field (CASSCF) methodology was used following by the multireference configuration interaction + single + double excitations (CASSCF + 1 + 2 = MRCISD) method. The CASSCF reference wavefunctions are built by distributing 10 [Mo ($4d^5 5s^1$) + C ($2s^2 2p^2$)] active electrons to ten orbital functions, one 5s and five 4d's on Mo + one 2s and three 2p's on C and the reference spaces range from 3080 ($d^5 \Pi$) to 7476 ($X^3 \Sigma^-$) configuration state functions (CSFs). Core correlation effects were considered by including the $4s^2 4p^6$ electrons of the molybdenum atom in the MRCI space. The corresponding MRCI spaces range from 2×10^{10} ($b^1 \Gamma$) to 4×10^{10} ($X^3 \Sigma^-$) CSFs. The construction of PECs becomes feasible after reducing these numbers by more than one or two orders of magnitude, respectively, via the internal contraction scheme [20, 21], icMRCISD. The Davidson correction for unlinked quadruples +Q [22] was used to ameliorate significant size nonextensivity problems. The potential energy curves are calculated at the icMRCISD(+Q) levels of theory. Bond distances, dissociation energies, relative energy ordering, and other spectroscopic constants are computed at all of the levels of theory employed. Note that in our analysis, spin-orbit effects have also been taken into consideration. Additionally, in each case, the bonding has been analyzed, which is visually represented through valence bond Lewis (vbL) diagrams. It is important to note that the bond order is determined by the number of chemical bonds, covalent or dative, between the atoms. A complete bond corresponds to a pair of electrons. The CASSCF wavefunctions display correct axial angular momentum symmetry along the molecular axis, i.e. $|\Lambda| = 0, 1, 2, \text{ etc.}$, while the symmetry of the MRCISD wavefunctions conforms to the symmetry species of the Abelian C_{2v} point group, i.e. A_1 (or A_2) for Δ and Γ , A_2 for Σ^- , and B_1 (or B_2) for Π . Finally, the spin-orbit coupling has been calculated employing the state interacting method for the $X^3 \Sigma^-$ and $A^3 \Delta$ states.[23] All calculations were performed by the MOLPRO suite of codes [23].

Finally, for the evaluation of the complete basis set limit (CBS) of the energetics, bond distances, spectroscopic values, *etc.*, two approaches were used.[24-27] In the first approach (I), all parameters are calculated in a series of basis sets and then the obtained values are extrapolated. In the second approach (II), the total energies are extrapolated to the CBS limit and then the spectroscopic constants are defined by the extrapolated CBS PEC. In both approaches the mixed Gaussian/exponential form (1) and the power function extrapolation scheme (2) are used. Note that both approaches and both extrapolation schemes have been successfully used in previous investigations.[24-27]

$$y_x = y_{\text{CBS}} + A e^{-(n-1)} + B e^{-(n-1)^2}, \quad (1)$$

$$y_x = y_{\text{CBS}} + B n^{-A}, \quad (2)$$

Here, A and B are fitted parameters and n corresponds to the size of the basis set.

III. EXPERIMENTAL

The experimental methods employed in resonant two-photon ionization (R2PI) spectroscopy have been described in detail elsewhere;[28] nuances of the method are more fully described in the Ph.D. dissertation of Dale J. Brugh. [29] An overview of the predissociation-based method for the measurement of bond dissociation energies is provided in our review article.[30] In the present investigation, a 1:1 V:Mo alloy disk was ablated using the second harmonic of a Nd:YAG laser (532 nm, ~18 mJ/pulse) to provide the source of Mo atoms. There is no benefit to using an alloy for this purpose; this was simply the most convenient source of Mo available in the laboratory. Because all recorded spectra are mass-analyzed, the presence of vanadium in the sample is irrelevant. A Smalley-type laser ablation source, [31] employing a carrier gas mixture of 4% CH₄ in helium at a pressure of 70 psig generated the MoC molecules. Although one might expect this gas mixture to also generate hydrogenated species such as MoCH, MoCH₂, *etc.*, there was no evidence of such species in the mass spectrum. The high-pressure gas expanded into a low-pressure chamber (~10⁻⁵ Torr), generating a supersonic expansion. Based on similar experiments on other molecules, the rotational temperature of the MoC molecules is expected to be roughly 30K or less.[32] A conical skimmer (0.5 cm diameter) then roughly collimated the expanding gases as they entered a second chamber held at ~10⁻⁶ Torr.

The second chamber housed a time-of-flight mass spectrometer (TOFMS) that was used to record mass-analyzed optical spectra using the R2PI process. Two lasers were utilized for the spectroscopic study: an optical parametric oscillator (OPO) laser that was scanned over the predissociation threshold of the MoC molecules and an exciplex laser operated on a KrF gas mixture, lasing at 248 nm. The tunable OPO laser was fired first, at the time of the greatest concentration of MoC molecules in the ion source of the TOFMS. The KrF laser was fired 80 ns later. Any ions produced were accelerated by a Wiley-McLaren electrode assembly,[33] separated by mass in the reflectron TOFMS,[34] and detected using a dual microchannel plate detector. The time-of-flight of the ions to the detector provided an unambiguous assignment of the mass of the ion. In this ionization scheme, ions could be generated by one of three processes. The molecules could absorb two OPO laser photons and be ionized by a one-color, two-photon process. Alternatively, they could either absorb two photons from the KrF laser (another one-color, two-photon process) or they could absorb one photon from the OPO laser and 80 ns later absorb one photon from the KrF laser, being ionized in a two-color, two-photon process. Because of the delay between the two laser pulses, the latter two ionization processes generate ions 80 ns after the first process. As a result, each isotopic modification of MoC is split into two peaks in the TOF mass spectrum, separated by 80 ns. By reducing the fluence of the KrF laser sufficiently to eliminate the ion signal due to absorption of two KrF laser photons, the second peak in the TOFMS signal provides signal dominated by the delayed two-color OPO +

KrF ionization process, which may therefore be selectively detected. The delay of 80 ns between the two laser pulses allows MoC molecules that are excited above the dissociation limit by the tunable OPO laser to have sufficient time to dissociate before ionization occurs. In previous studies of molecules where the ground separated atom limit generates few potential energy curves, such as CrO and YbO, we have found that such a delay is necessary to obtain a sharp predissociation threshold that is indicative of the bond dissociation energy.[35-36] In the case of MoC, there was no discernible difference in the predissociation threshold between the signal recorded by the OPO + OPO one-color R2PI spectrum and the OPO + KrF two-color R2PI spectrum, demonstrating that predissociation occurs on a nanosecond to subnanosecond time scale as soon as the BDE is exceeded.

IV. EXPERIMENTAL RESULTS

Diatomic $^{98}\text{Mo}^{12}\text{C}$ was monitored for this study because it is the most abundant isotopologue (23.86% natural abundance) and there is a convenient gap in the mass spectrum between this species and the next heavier isotopologue, $^{100}\text{Mo}^{12}\text{C}$ (we neglect $^{98}\text{Mo}^{13}\text{C}$, as its natural abundance is only 0.268%). This gap in the mass spectrum allowed us to conveniently monitor $^{98}\text{Mo}^{12}\text{C}^+$ ions produced by the delayed two-color, two-photon ionization scheme without interference from other isotopologues. Figure 1 displays the two-color, two-photon ionization spectrum over the range 39,000-43,000 cm^{-1} obtained using the 80 ns delayed OPO + KrF ionization process. Below 41,425 cm^{-1} , the spectrum displays a complicated quasicontinuum that defies spectroscopic analysis. At 41,425 cm^{-1} , however, the ion signal rapidly drops to baseline, indicating that the molecule dissociates within the 80 ns period prior to the KrF ionization laser pulse. Accordingly, we assign 41,425 cm^{-1} as the bond dissociation energy. The horizontal bar atop the black arrow in Figure 1 designates the error ($\pm 25 \text{ cm}^{-1}$) assigned to the measurement. The assigned error encompasses the linewidth of the excitation laser $\sim 10 \text{ cm}^{-1}$, the rotational temperature of the molecules, possible calibration error in the wavenumber axis, and the subjective sharpness of the drop in cation signal to baseline. Calibration of the wavenumber axis was accomplished by simultaneously recording the optical spectrum of atomic ^{98}Mo and comparing the observed atomic spectrum with atomic data compiled by NIST.[37] The only previous measurement of the MoC BDE is the Knudsen effusion mass spectrometric study, which obtained 4.95(17) eV.[5] Here we report the assigned error limit in parentheses, in units of the last reported digit. Our measurement, 5.136(3) eV, shifts this value higher by 0.19 eV and decreases the error limit by a factor of 50.

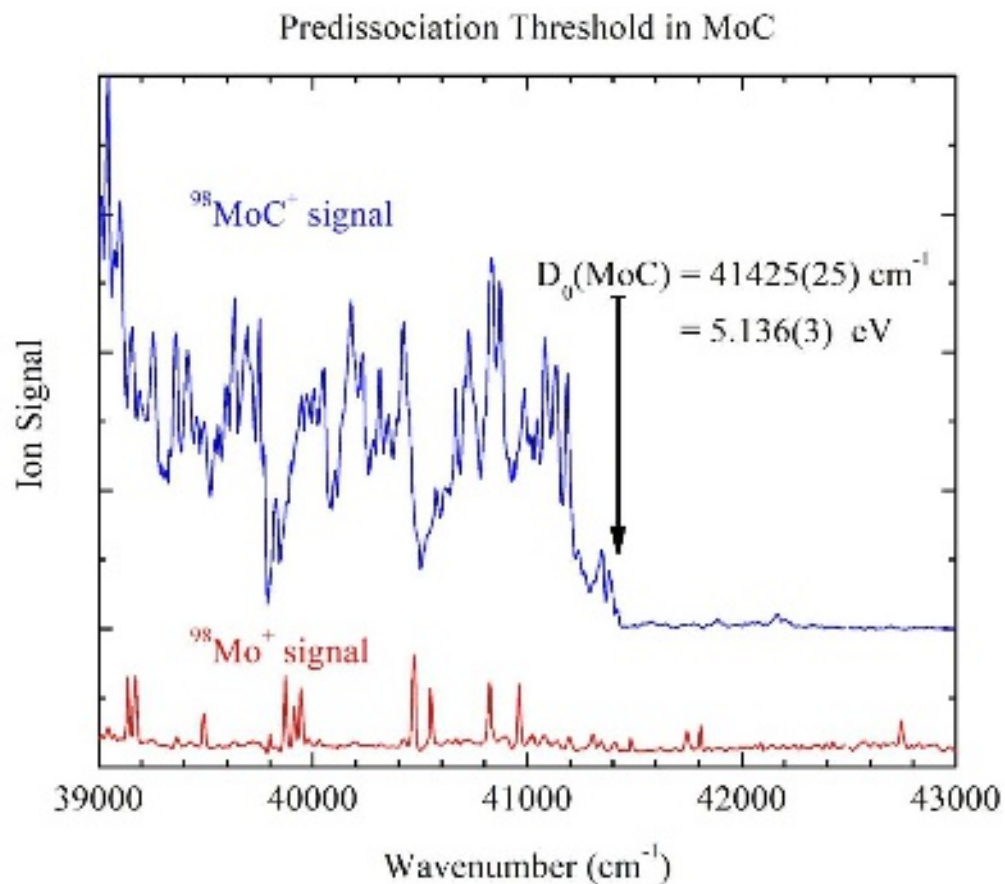


Figure 1. Delayed OPO + KrF R2PI spectrum of MoC (upper blue trace) in the energetic vicinity of its predissociation threshold at $41,425(25) \text{ cm}^{-1}$. Mo atomic transitions (lower red trace) were used to calibrate the spectrum.

V. COMPUTATIONAL RESULTS AND DISCUSSION

The seven lowest energy states, $X^3\Sigma^-$, $A^3\Delta$, $a^1\Gamma$, $b^5\Sigma^-$, $c^1\Delta$, $d^1\Sigma^+$, and $e^5\Pi$, were calculated via multireference methodologies to provide highly precise electronic state data and to study the chemical bonding. Their potential energy curves are plotted in Figure 2. The $b^5\Sigma^-$ and $e^5\Pi$ states correlate to atomic ground state products, $\text{Mo} (^7\text{S}_g) + \text{C} (^3\text{P}_g)$, while the $X^3\Sigma^-$, $A^3\Delta$, $a^1\Gamma$, $c^1\Delta$, and $d^1\Sigma^+$, correlate to $\text{Mo} (^5\text{S}_g) + \text{C} (^3\text{P}_g)$, $\text{Mo} (^5\text{D}_g) + \text{C} (^3\text{P}_g)$, and $\text{Mo} (^3\text{G}_g) + \text{C} (^3\text{P}_g)$ (singlet states), respectively. Despite having different spin multiplicities, these five states all exhibit the same quadruple bonding.

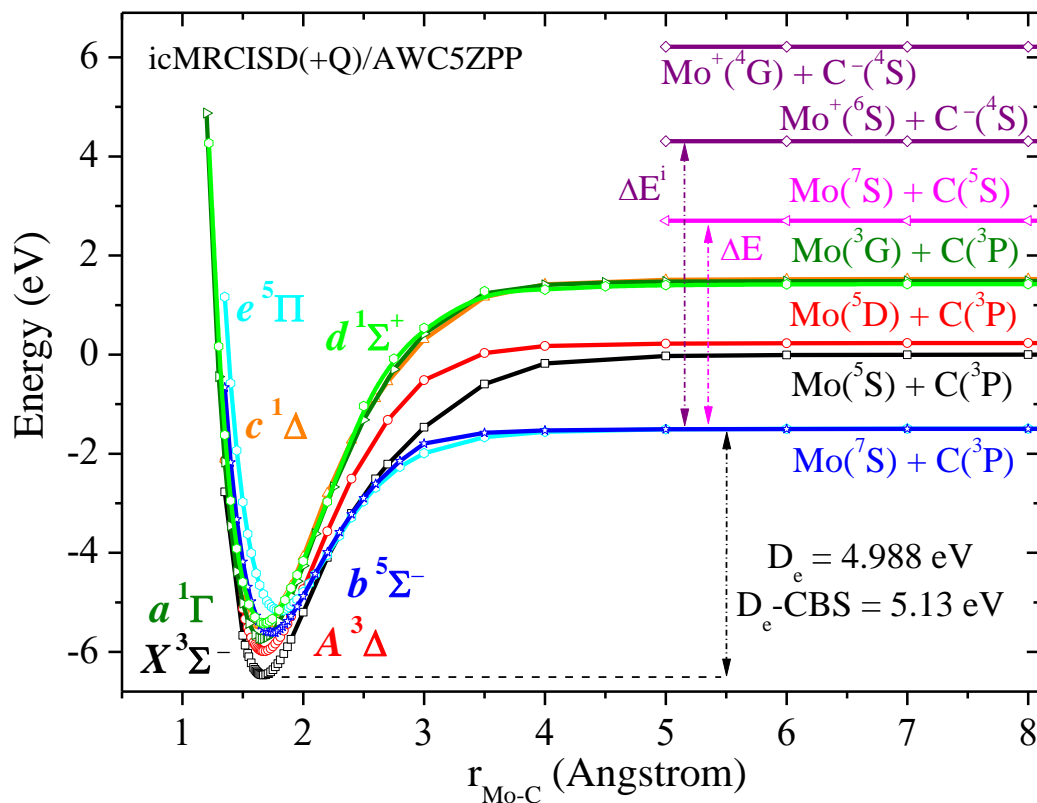
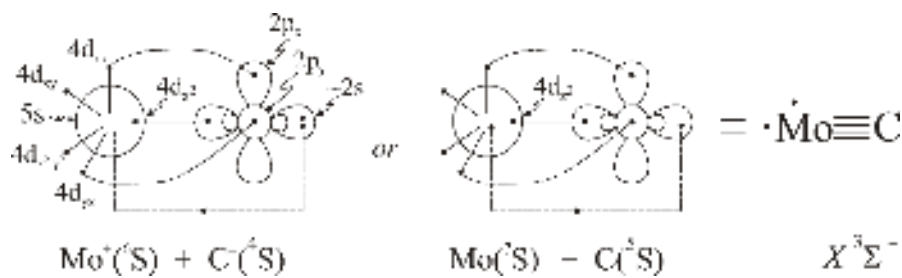


Figure 2. Potential Energy Curves of the calculated states of MoC at the C-MRCISD(+Q)/aug-cc-pwCV5Z(-PP) computational level. The Mo (5S_g) + C (3P_g) limit, to which the $X^3\Sigma^-$ state correlates, is used to define the zero of energy for this figure.

A. Electronic Structure and Chemical Bonding

$X^3\Sigma^-$ state: The ground state of MoC is separated from the remaining states by approximately 4000 cm^{-1} .^[6,9] It dissociates to the Mo (5S_g) + C (3P_g) excited separated atom limit, as displayed in Figure 2. At the potential energy minimum, the leading CASSCF configuration is $\langle X^3\Sigma^- \rangle = 0.91|1\sigma^2 2\sigma^2 1\delta_+^1 1\pi_x^2 1\pi_y^2 1\delta_-^1 \rangle$ and the X state has ionic character. Mulliken, NBO analysis, and Hirshfeld population analysis show that the C atom has a negative charge. The Mulliken negative charge depends on the basis set and ranges from -0.33 to -0.72 electrons, while the NBO, Hirshfeld H-charges and CM5 charges are independent of basis set; their values are -0.34, -0.35, and -0.52, respectively. All population analysis methods show the occupation in the 5s orbital of Mo at the equilibrium bond length to be less than 0.2 electrons, indicating that the electronic wavefunction at the potential energy minimum is dominated by an ionic structure, *i.e.*, $\text{Mo}^+ + \text{C}^-$. The NBO and Hirshfeld charges are the same and are considered to be the most accurate. Regarding the Mulliken populations, the icMRCISD/AVTZDK and C-icMRCISD/AWC5Z(PP) methodologies provide charges in agreement with the NBO data. The corresponding atomic distributions (Mo/C) are:

$5s^{0.14}5p_z^{0.10}5p_x^{0.01}5p_y^{0.01}4d_{z^2}^{1.15}4d_{xz}^{1.05}4d_{yz}^{1.05}4d_{x^2-y^2}^{0.99}4d_{xy}^{0.99}$ / $2s^{1.85}2p_z^{0.79}2p_x^{0.91}2p_y^{0.91}$ and
 $5s^{0.20}5p_z^{0.09}5p_x^{0.02}5p_y^{0.02}4d_{z^2}^{1.26}4d_{xz}^{1.06}4d_{yz}^{1.06}4d_{x^2-y^2}^{0.99}4d_{xy}^{0.99}$ / $2s^{1.75}2p_z^{0.71}2p_x^{0.90}2p_y^{0.90}$, respectively. The number of electrons in the Mo 5s orbital as a function of internuclear distance is depicted in Figure 3a; at the potential energy minimum, the 5s orbital is almost empty. At internuclear distances between 1.5 and 3.5 Å, the nature of the intermolecular interaction becomes mainly ionic. The X state dissociates to Mo (5S_g) + C (3P_g), and it seems that avoided crossings exist near 3.5 and 2.5 Å, see Figure S1 of the Supplementary Material. In Figure 3a, a significant reduction in the occupancy of the 5s atomic orbital of Mo is observed as the internuclear separation contracts from 4 to 3.5 Å [$Q_{5s}(\text{Mo}) = 0.81 \rightarrow Q_{5s}(\text{Mo}) = 0.27$]. This is an indication of the transition to the ionic structure, $\text{Mo}^+(\text{^6S}_g) + \text{C}^-(\text{^4S}_u)$, from the covalent one, $\text{Mo}(\text{^5S}_g) + \text{C}(\text{^3P}_g)$, as the internuclear separation is decreased. There is also the possibility that the bonds could be formed from $\text{Mo}(\text{^7S}_g) + \text{C}(\text{^5S}_u)$, where the C atom is excited, but the $1\sigma^2$ ($5s^1-2s^1$) bond would be very polar, *i.e.*, almost 0.8 electrons being transferred to the C atom, so that the $1\sigma^2$ electron pair is located on the carbon. Regardless of whether the bonding results from $\text{Mo}^+(\text{^6S}_g; 4d^5) + \text{C}^-(\text{^4S}_u; 2s^2 2p^3)$ or from $\text{Mo}(\text{^7S}_g; 5s^1 4d^5) + \text{C}(\text{^5S}_u; 2s^1 2p^3)$, there is an intense ionic character which is corroborated by the large calculated dipole moment of about 6 Debye, see Table 2. The high ionic character is also evident in the measured dipole moment of 6.07 ± 0.18 D,[12] which is in good agreement with our computed value. Finally, it should be noted that Denis and Balasubramanian [10] also describe the bond in the ground state as polar, with an electron transfer from Mo(5s) to C(2p) which results in Mo^+-C^- ionic character and then a back transfer from C to Mo(4d).[10]



Scheme 1: Valence Bond Lewis diagram of the ground $X^3\Sigma^-$ state of MoC.

To sum up, based on the leading CSF, the atomic Mulliken distributions, and the molecular orbital composition, the $X^3\Sigma^-$ state is quadruple-bonded, *i.e.*, $1\sigma^2 2\sigma^2 1\pi_x^2 1\pi_y^2$, as indicated in the vbL diagram of Scheme 1 and Table 3. The quadruple bond is formed by two π^2 covalent bonds, *i.e.*, $1\pi_x^2 = 4d_{xz}^1-2p_x^1$ and $1\pi_y^2 = 4d_{yz}^1-2p_y^1$, one σ^2 covalent bond, *i.e.*, $2\sigma^2 = 4d_{z^2}^1-2p_z^1$, and one $1\sigma^2$ bond, where significant 5s-4d_{z2} hybridization exists, see Table 3. If we consider the bond to be formed between ions, $\text{Mo}^+(\text{^6S}_g) + \text{C}^-(\text{^4S}_u)$, then the $1\sigma^2$ bond is dative, *i.e.* $5s^0 \leftarrow 2s^2$. Alternatively, if we

consider that the bonding is formed between $\text{Mo}(^7S_g) + \text{C}(^5S_u)$, then the $1\sigma^2$ bond is covalent, $5s^1 \leftarrow 2s^1$. However, the molecular orbitals (Table 3 and Figure 4) indicate that the 1σ orbital is mainly localized on carbon, causing the bonding to be mainly ionic, as $\text{Mo}^+ + \text{C}^-$. The molecular orbitals (MOs) of the $X^3\Sigma^-$ state are depicted in Figure 4.

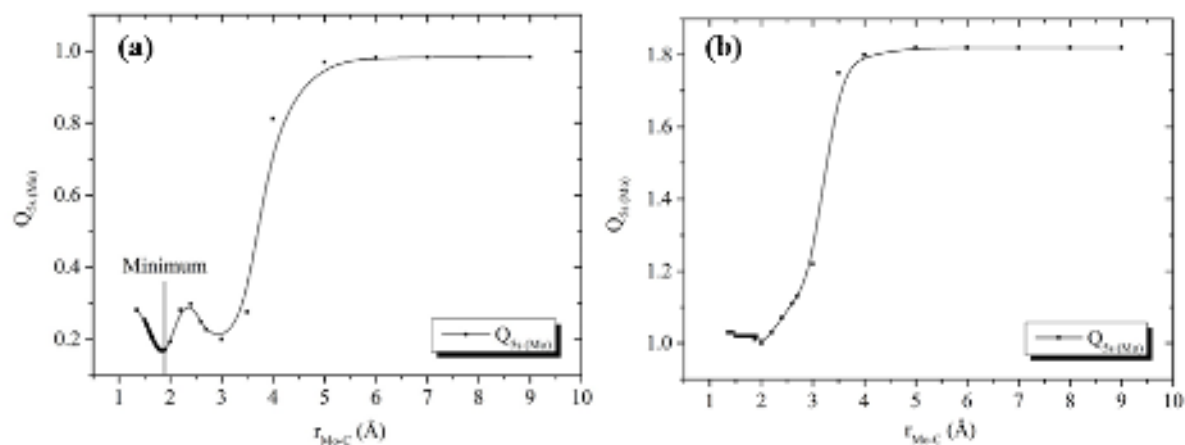


Figure 3: Occupancy of the Mo 5s orbital as a function of the internuclear distance, $r_{\text{Mo-C}}$ a: ($X^3\Sigma^-$) and b: ($1^3\Delta$).

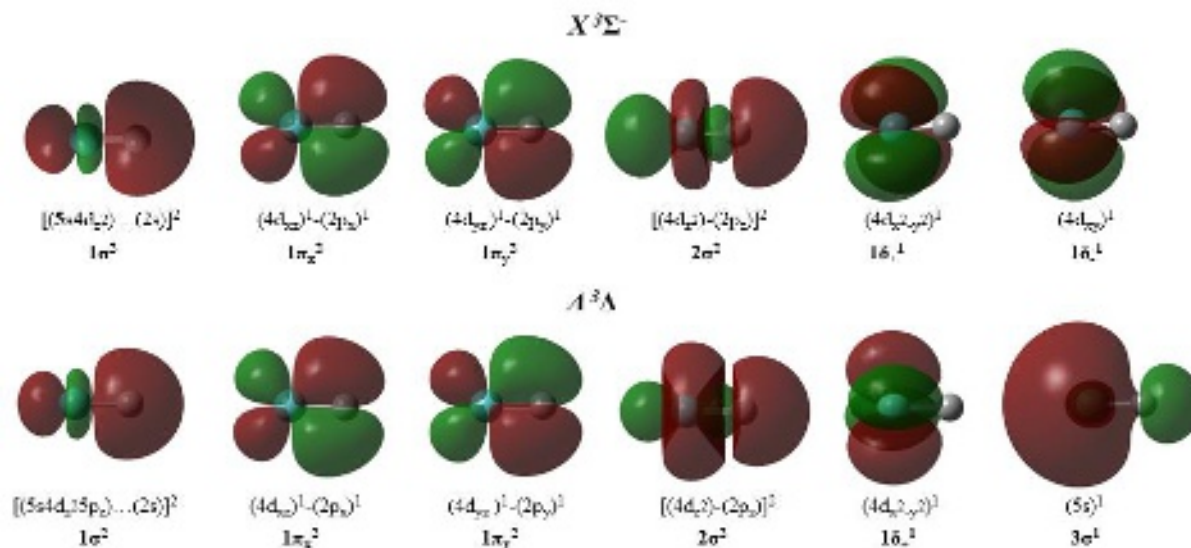
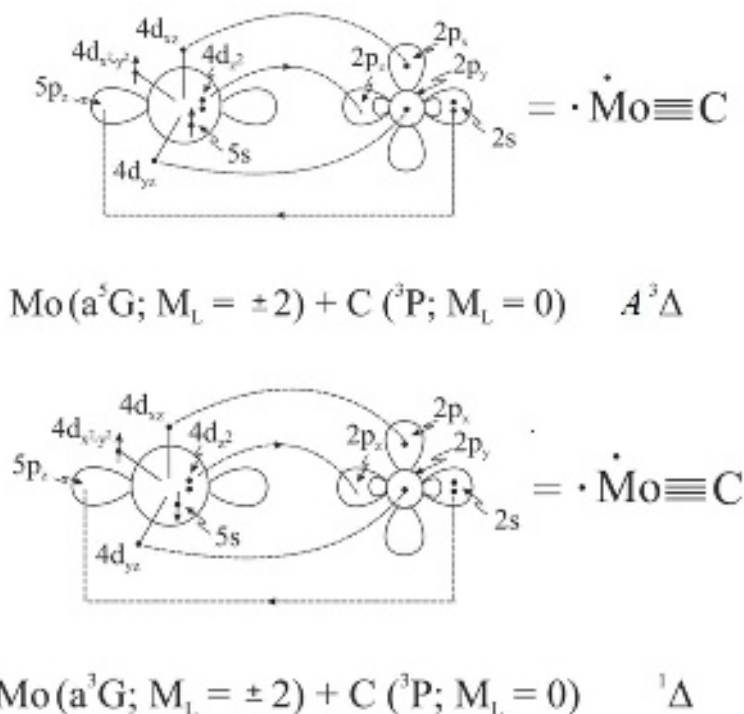


Figure 4. MOs of the $X^3\Sigma^-$ and $A^3\Delta$ states. The atomic orbitals with the main contribution are given for each MO.

$A^3\Delta$ and $c^1\Delta$ states: The first excited state, $A^3\Delta$, dissociates to $\text{Mo}(a^5D_g, \pm 2; 4d^45s^2) + \text{C}(^3P_g, 0)$, but there is an avoided crossing at about 3 Å, and as a result at the potential energy minimum this state corresponds to $\text{Mo}(a^5G_g, \pm 2; 4d^55s^1) + \text{C}(^3P_g, 0)$. The leading equilibrium CASSCF

configuration is $|A_1^3\Delta\rangle = 0.93\left(\frac{1}{\sqrt{2}}|1\sigma^2 2\sigma^2 3\sigma^1(1\delta_+^1 + 1\delta_-^1)1\pi_x^2 1\pi_y^2\rangle\right)$ and the corresponding linear combination of the atomic orbitals is given in Table 3. The ensuing atomic Mulliken populations (Mo/C) at the icMRCISD/AVTZDK level of theory are $5s^{0.86}5p_z^{0.18}5p_x^{0.02}5p_y^{0.02}4d_{z^2}^{1.20}4d_{xz}^{1.15}4d_{yz}^{1.15}4d_{x^2-y^2}^{0.99}4d_{xy}^{0.03}/2s^{1.84}2p_z^{0.84}2p_x^{0.83}2p_y^{0.83}$

The fourth excited state, $c_1^1\Delta$, has also been investigated. It dissociates to Mo (a^3G_g) + C (3P_g), as shown in Figure 2. Note that for the Mo atom, the $^3P_{0g}$ level is lower than the $^3D_{1g}$ by 323 cm^{-1} and is lower than the $^3G_{3g}$ atomic state by 341 cm^{-1} ; however, for the J -averaged atomic states, the 3G_g term is lower than 3D_g by 81 cm^{-1} and lower than 3P_g by 1236 cm^{-1} .^[37] The main equilibrium CASSCF configuration is $|c_1^1\Delta\rangle = 0.93\left(\frac{1}{\sqrt{2}}|1\sigma^2 2\sigma^2 3\sigma^1(1\delta_+^1 + 1\delta_-^1)1\pi_x^2 1\pi_y^2\rangle\right)$ and the Mulliken populations (Mo/C) at the icMRCISD/AVTZDK level of theory are $5s^{0.97}5p_z^{0.16}5p_x^{0.02}5p_y^{0.02}4d_{z^2}^{1.22}4d_{xz}^{1.12}4d_{yz}^{1.12}4d_{x^2-y^2}^{0.98}4d_{xy}^{0.04}/2s^{1.80}2p_z^{0.81}2p_x^{0.86}2p_y^{0.86}$



Scheme 2: Valence Bond Lewis diagrams of the $A_1^3\Delta$ and $c_1^1\Delta$ states of MoC for the A_1 component. The A_2 component has the $4d_{xy}$ orbital single occupied instead of $4d_{z^2-y^2}$.

The bonding in both Δ states is captured by the vBL diagrams displayed in Scheme 2, based on the leading CSFs, the atomic Mulliken distributions, and the molecular orbital compositions. The bonding scheme in these two states is essentially the same, consisting of two σ^2 and two π^2 bonds,

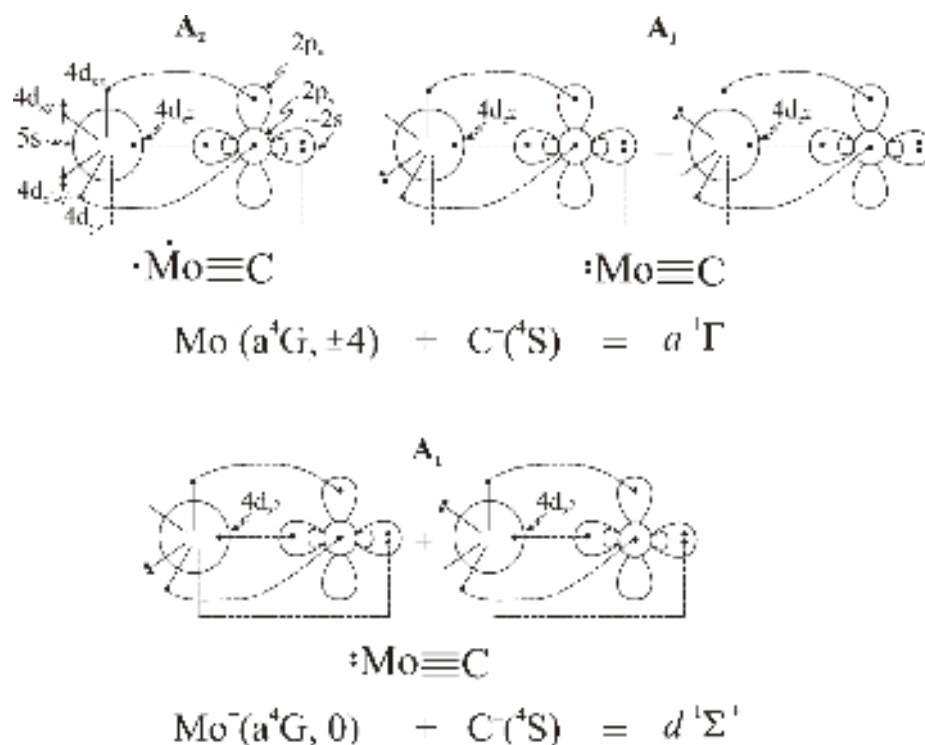
see Scheme 2 and Figure 4. The MO plots of the ${}^1\Delta$ state are quite similar to those of the $A^3\Delta$ state. The only significant difference between them lies in the spin directions of the 5s and $4d_{x^2-y^2}$ electrons of Mo. In the $A^3\Delta$ state, these electrons are high-spin coupled, giving rise to a triplet state. In the ${}^1\Delta$ state, these electrons are low-spin coupled, giving rise to an open-shell singlet state. In both states, the C atom is in its ground state ${}^3P(0)$ forming two π^2 covalent bonds, $4d_{xz}^1-2p_x^1$ and $4d_{yz}^1-2p_y^1$. Furthermore, two dative σ^2 bonds are formed, namely $1\sigma^2: 5s4d_05p_z^0 \leftarrow 2s^2$ and $2\sigma^2: 4d_{z^2}^2 \rightarrow 2p_z^0$. About $0.2 e^-$ are transferred from C to Mo via the $1\sigma^2$, where there is a $5s4d_05p_z$ hybridization, while $0.3 e^-$ are transferred via the two π bonds, and about $0.8 e^-$ are transferred back via the $2\sigma^2$ to the C atom. A significant reduction of the occupation of the 5s atomic orbital of Mo occurs near at 3.5 \AA [$Q_{5s(\text{Mo})} = 1.75 \rightarrow Q_{5s(\text{Mo})} = 1.22$] is observed, see Figure 3b. This observation demonstrates that while the $A^3\Delta$ state dissociates to an Mo atom in its second excited state ($a^5D_g; 4d^45s^2$), at the potential energy minimum the molecular state derives from the ${}^5G_g (4d^55s^1)$ atomic state, due to an avoided crossing. Furthermore, the observed $5s4d_{z^2}5p_z$ hybridization affects the depiction of 3σ orbital (Figure 4 and Table 3), which seems like a weak antibonding orbital. However, it does not weaken the bond and does not reduce the bond order. Note, that the dissociation energy of the $A^3\Delta$ and $c^1\Delta$ states with respect to the adiabatic atomic products are 6.224 eV and 7.000 eV, i.e., similar to the corresponding value of the ground state, i.e., 6.472 eV, see Table 2 and discussion below. Finally, it should be noted that even though both Δ states have the same electronic configuration and bonding, the spin plays a role in their geometry, i.e., it results in a shorter bond distance in the $c^1\Delta$ state than in the $A^3\Delta$ state by 0.01 \AA , see Table 2.

The main difference between these two Δ states and the ground $X^3\Sigma^-$ state is that the 5s orbital is singly occupied in the two Δ states, while in the X state, it is nearly empty. Furthermore, the dipole moments of the Δ states are half of the dipole moment of the X state, which has been characterized as polar; see the further discussion of dipole moments below. Finally, another issue that should be highlighted pertains to the bond multiplicity of the calculated states of MoC. In all cases, a quadruple bond comprising two σ^2 and two π^2 bonds is formed between Mo and C. However, it should be noted that while the $2\sigma^2$ is clearly a covalent bond in the $X^3\Sigma^-$ state (similar coefficient for the $4d_{z^2}$ and $2p_z$ atomic orbitals) and a dative bond in the $A^3\Delta$ and ${}^1\Delta$ state (larger coefficient for the $4d_{z^2}$ than the $2p_z$ atomic orbital), the $1\sigma^2$ bond is in all cases weak, with electron density mainly localized in the 2s orbital of C.

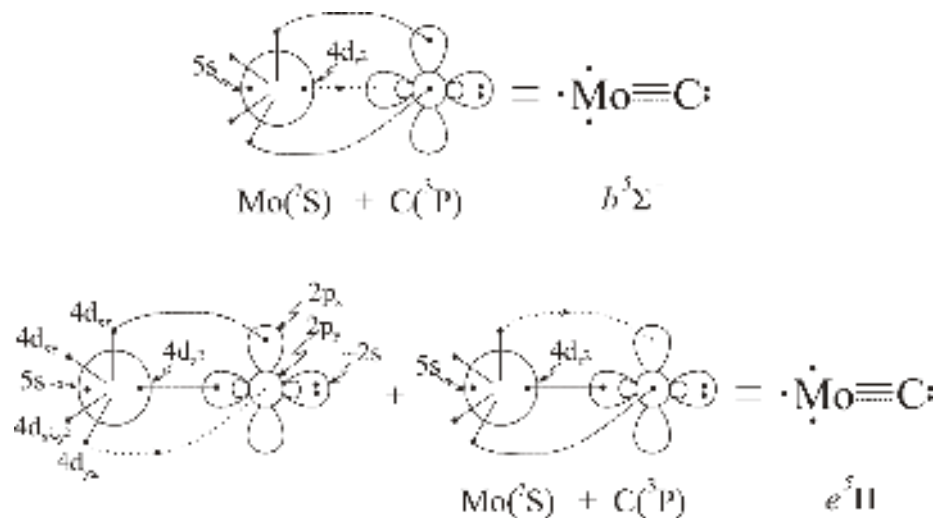
$a^1\Gamma$ and $d^1\Sigma^+$ states: Both excited states dissociate to $\text{Mo}(a^3G_g, \pm 4; 4d^55s^1) + \text{C}({}^3P_g, 0)$, while there is an avoided crossing at about 3.5 \AA for both states. As a result, at the equilibrium position, their electronic structure derives from $\text{Mo}^+(a^4G_g, \pm 4; 4d^5) + \text{C}^-({}^4S_u)$, i.e., the states are formed

This is the author's peer reviewed, accepted manuscript. However, the online version of record will be different from this version once it has been copyedited and typeset. PLEASE CITE THIS ARTICLE AS DOI: 10.1063/1.5031174

between ions. The leading equilibrium CASSCF configurations are: $|a^1\Gamma\rangle = 0.94\left(|1\sigma^2 2\sigma^2 1\pi_x^2 1\pi_y^2 (1\delta_+^1 1\delta_-^1 + 1/\sqrt{2}(1\delta_+^2 - 1\delta_-^2))\rangle\right)$ and $|d^1\Sigma^+\rangle = 0.68|1\sigma^2 2\sigma^2 1\pi_x^2 1\pi_y^2 (1\delta_+^2 + 1\delta_-^2)\rangle$. The contributions of the atomic orbitals to the MOs is given in Table 3. The resulting atomic Mulliken populations (Mo/C) of the $a^1\Gamma$ state are $5s^{0.17}5p_z^{0.10}5p_x^{0.01}5p_y^{0.01}4d_{z^2}^{1.28}4d_{xz}^{1.07}4d_{yz}^{1.07}4d_{x^2-y^2}^{1.00}4d_{xy}^{1.00}/2s^{1.73}2p_z^{0.71}2p_x^{0.90}2p_y^{0.90}$ at the icMRCISD/AVTZDK level of theory. The bonding is depicted in Scheme 3, where both A_1 and A_2 components are presented. A quadruple bond $\sigma^2\sigma^2\pi^2\pi^2$ is formed, *i.e.*, two covalent π^2 bonds: $4d_{xz}^1-2p_x^1$ and $4d_{yz}^1-2p_y^1$, one covalent σ^2 bond: $4d_{z^2}^1-2p_z^1$ and one dative σ^2 bond: $5s5p_z^0\leftarrow 2s^2$. About $0.2 e^-$ are transferred via the π bonds and about $0.5 e^-$ via the σ^2 bonds from C^- to Mo^+ . Overall, the carbon atom is negatively charged at the equilibrium position, $-0.36 e$, while in the $2.7-3.0 \text{ \AA}$ range where the bonds have not completely formed, the charge is about $-0.6 e$. It should be mentioned that the $d^1\Sigma^+$ state presents almost the same charges and the same bonding with the $a^1\Gamma$. Both states have the shortest bond length at 1.664 \AA at the C-icMRCISD+Q/AWC5ZPP level, *i.e.*, 0.009 \AA shorter than the X state, see Table 2. Overall, both states are very similar to the ground $X_{\Sigma}^3\Sigma^-$ state, however the 1δ electrons are coupled to give low spin ($S=0$).



Scheme 3: Valence Bond Lewis diagrams of the $a^1\Gamma$ and $d^1\Sigma^+$ states of MoC.



Scheme 4: Valence Bond Lewis diagrams of the $b^5\Sigma^-$ and $e^5\Pi$ states of the MoC molecule.

$b^5\Sigma^-$ and $e^5\Pi$ states: The third and sixth excited states, $b^5\Sigma^-$ and $e^5\Pi$, dissociate to ground state atoms, Mo ($^7\text{S}_g$) + C ($^3\text{P}_g$), as shown in Figure 2. Both states keep this character at the equilibrium position. Their main equilibrium CASSCF configurations are

$$|b^5\Sigma^- \rangle = 0.92 |1\sigma^2 2\sigma^1 3\sigma^1 1\pi_x^2 1\pi_y^2 1\delta_+^1 1\delta_-^1 \rangle \text{ and}$$

$|e^5\Pi \rangle = 0.92 \left(\frac{1}{\sqrt{2}} |1\sigma^2 2\sigma^2 3\sigma^1 (1\pi_x^2 1\pi_y^1 + 1\pi_x^1 1\pi_y^2) 1\delta_+^1 1\delta_-^1 \rangle \right)$. The bonding is depicted in Scheme 4. Two and a half bonds are formed in both states, i.e., $\sigma^1\pi^2\pi^2$ ($b^5\Sigma^-$) and $\sigma^2\pi^2\pi^1$ ($e^5\Pi$). The Mulliken populations (Mo/C) at the icMRCISD/AVTZDK level of theory are:

$$b^5\Sigma^-: 5s^{0.85} 5p_z^{0.11} 5p_x^{0.02} 5p_y^{0.02} 4d_{z^2}^{0.77} 4d_{xz}^{0.99} 4d_{yz}^{0.99} 4d_{x^2-y^2}^{0.99} 4d_{xy}^{0.99} / 2s^{1.64} 2p_z^{0.65} 2p_x^{0.96} 2p_y^{0.96}$$

$e^5\Pi: 5s^{0.83} 5p_z^{0.10} 5p_x^{0.05} 5p_y^{0.02} 4d_{z^2}^{1.11} 4d_{xz}^{1.01} 4d_{yz}^{0.58} 4d_{x^2-y^2}^{0.99} 4d_{xy}^{0.99} / 2s^{1.89} 2p_z^{1.00} 2p_x^{0.94} 2p_y^{0.41}$. Overall, 0.3 e^- are transferred from Mo to the C atom. Note that there is a $5s4d_05p_z$ hybridization in Mo and a $2s2p_z$ in C. In these states there is a weak interaction between the $2s^2$ orbital and the $5s4d_05p_z$ hybrid orbital on Mo, but the donation of $2s^2$ electrons to Mo via this orbital is counteracted by partial electron transfer back to carbon through the σ frame, via the $2\sigma^1$ electron in the $b^5\Sigma^-$ term and the $2\sigma^2$ electrons in the $e^5\Pi$ term. The weak bonding interaction of the $1\sigma^2$ electrons in these states is not sufficient to consider that they form a bond. Finally, it should be noted, even though the $a^1\Gamma$ state is formed from ions, $\text{Mo}^+(\text{a}^4\text{G}_g, \pm 4; 4d^5) + \text{C}^-(^4\text{S}_u)$, while the $b^5\Sigma^-$ and $e^5\Pi$ states result from the atomic ground state products, $\text{Mo}(^7\text{S}_g) + \text{C}(^3\text{P}_g)$, the carbon in equilibrium has a charge of about -0.3 e , due to the electron charge transfer in the bonds.

B. Dissociation Energies and Geometry: As we can see from Table 2, the correlation of the $4s^24p^6$ electrons of Mo and $1s^2$ electrons of C reduces the Mo-C bond distance by 0.009 Å and

increases the dissociation energy with respect to the adiabatic atomic products by up to 0.25 eV. For the ground state, $X_{\text{e}}^3\Sigma^-$, at our best methodology, *i.e.*, C-icMRCISD(+Q)/AWCV5Z(PP), the Mo-C bond distance is calculated at 1.673 Å and the dissociation energy with respect to the adiabatic products, Mo (5S_g) + C (3P_g), is 6.472 eV, while with respect to the atomic ground states, Mo (7S_g) + C (3P_g), is 4.988 eV. The $A^3\Delta$, $a^1\Gamma$, and $c^1\Delta$, and $d^1\Sigma^+$ states have similar bond distances as the X state, *i.e.*, 1.677 Å, 1.664 Å, 1.666 Å, and 1.664 Å, respectively. They lie 0.48 eV, 0.73 eV, 1.00 eV, and 1.06 eV above the ground state, respectively, and their dissociation energies with respect to the adiabatic atomic products are 6.224 eV, 7.231 eV, 7.000 eV, and 6.942 eV at the C-icMRCISD(+Q)/AWCV5Z(PP) level of theory, while the corresponding dissociation energy of the ground state is 6.472 eV. These large dissociation energies justify the assignment of quadruple bonding in these states. Finally, the $b^5\Sigma^-$ ($\sigma^1\pi^2\pi^2$) and $e^5\Pi$ ($\sigma^2\pi^2\pi^1$) states that correlate to the atomic ground state products, Mo (7S) + C (3P), have dissociation energies of 4.121 eV and 3.671 eV and bond lengths of 1.739 Å and 1.807 Å, respectively. In these states a bonding 2σ or 1π electron has been promoted to the nonbonding 3σ orbital, significantly increasing the bond length and reducing the adiabatic bond dissociation energy.

For the ground state, the CBS limits of the Mo-C bond distance and dissociation energy with respect to the atomic ground state products were calculated via two approaches, *i.e.*, (I): the quantities are calculated in a series of basis sets and then these values are extrapolated and (II) the total energies are extrapolated to the CBS limit and then the spectroscopic constants are defined by the extrapolated CBS PEC, using either the mixed Gaussian/exponential scheme (1) or the power function extrapolation scheme (2). Thus, the CBS limits are $R_e = 1.670$ Å and $D_e(D_0) = 5.07(5.01)$ eV, as provided in Table 4. Taking into account the correlation energy difference between the DK method and the relativistic pseudopotential, our final $D_e(D_0)$ values are 5.13(5.06) eV. Experimentally, a thermochemical value of $D_0 = 4.95 \pm 0.17$ eV was obtained in 1981 using the Knudsen effusion mass spectrometric method.[5] Here we report a predissociation-based measurement that greatly reduces the error limit, providing $D_0(\text{MoC}) = 5.136 \pm 0.003$ eV (Figure 1). This is in excellent agreement with our calculated value, which underestimates the experimental value by only 0.07 eV.

The PECs of the seven calculated states are depicted in Figure 2. For the sake of completeness, the ionic asymptote has also been plotted, based on the calculations performed for the ionization potential of Mo and the electron affinity of C. The energy difference, ΔE^i , between the ground state asymptote and the ionic asymptote is equal to I.P. (Mo) – E.A. (C), *i.e.* 5.789 eV, ($=\Delta E^i$ in Figure 2). More specifically, the ionization potential of Mo was calculated to be 6.981 eV, while the electron affinity of C was computed to be 1.192 eV. These theoretical values agree well with the corresponding experimental ones, *i.e.* 7.09243(4) eV [37] and 1.262114(44) eV [37], respectively. Additionally, the

$\text{Mo}(^7\text{S}_g) + \text{C}(^5\text{S}_u)$ asymptote has also been plotted. The excitation energy of $\text{C}(^5\text{S}_u \leftarrow ^3\text{P}_g)$ is calculated at 4.184 eV at C-iMRCISD/AWC5Z, in excellent agreement with the experimental value of 4.1826 eV [37]. Thus, for the $X^3\Sigma^-$ state, the calculated dissociation energy, D_e , at the CBS limits is: i) 5.13 eV with respect to the atomic ground state products, $\text{Mo}(^7\text{S}_g) + \text{C}(^3\text{P}_g)$; ii) 6.61 eV with respect to the adiabatic products, $\text{Mo}(^5\text{S}_g) + \text{C}(^3\text{P}_g)$; iii) with respect to the states of the atoms in the molecule at the equilibrium position is 9.31 eV (considering the atomic states $\text{Mo}(^7\text{S}_g) + \text{C}(^5\text{S}_u)$) or 10.92 eV (with respect to the ionic products, $\text{Mo}^+(^6\text{S}_g) + \text{C}(^4\text{S}_u)$ since only $0.2 e^-$ of the $1\sigma^2$ bond is on Mo).

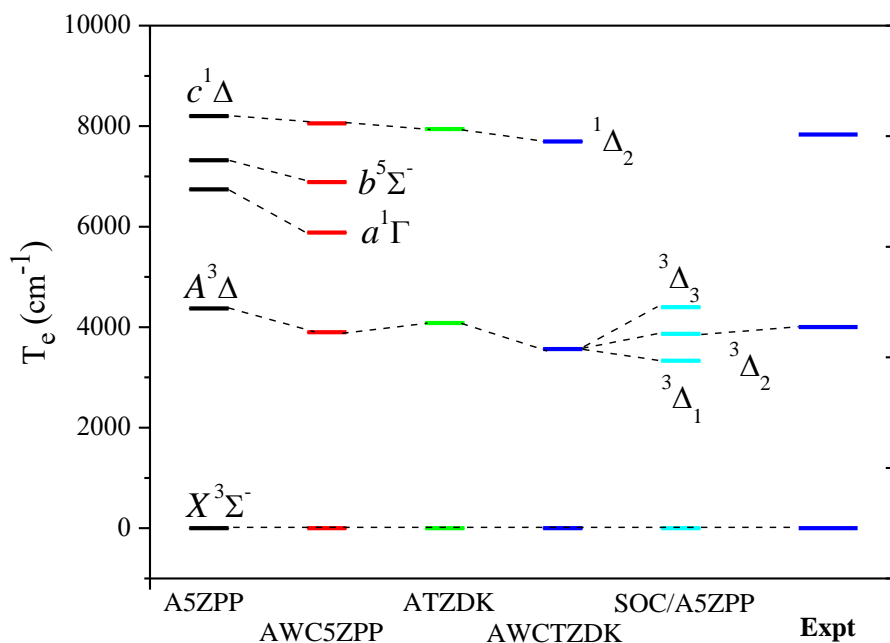


Figure 5. Relative icMRCISD+Q energy differences at various basis sets. Spin-orbit coupling corrections have been included.

Finally, the spin orbit coupling (SOC) has been calculated. The relative icMRCISD energy differences at various basis sets and the SOC have been also included, see Figure 5. The excited electronic states $A^3\Delta_1$, $A^3\Delta_2$, $A^3\Delta_3$, $a^1\Gamma_4$, $b^5\Sigma_2^-$, and $d^1\Delta_2$ are calculated to lie at 3334 cm^{-1} , 3899 cm^{-1} , 4398 cm^{-1} , 5883 cm^{-1} , 6886 cm^{-1} , and 8057 cm^{-1} , respectively, in excellent agreement with the available experimental values of DaBell *et al.*, [9] 4002.5 cm^{-1} ($A^3\Delta_2$) and 7834 cm^{-1} ($d^1\Delta_2$) respectively, see Figure 5.

C. Dipole Moment values: The dipole moment values have been calculated as expectation values and *via* the finite field method. Both methods predict similar values, see Table 1. The largest differences are obtained for the $^5\Sigma^-$ state, with differences up to 0.4 D (C-MRCISD/ AWC5ZPP)

between expectation values and the finite field result. We consider our best results to be the expectation values [38] at the C-MRCISD/AWCV5Z(-PP) level. Thus, our final values are 5.88 D ($X^3\Sigma^-$), 3.02 D ($A^3\Delta$), 5.82 D ($a^1\Gamma$), 2.52 D ($b^5\Sigma^-$), 2.29 D ($c^1\Delta$), 5.93 D ($d^1\Sigma^+$), and 3.11 D ($e^5\Pi$). The large value in the X state is in accord with its polar character and matches quite well with the experimental value of 6.07 ± 0.18 D.[12] It should be noted that the ground $X^3\Sigma^-$ state of the isovalent CrC molecule also has a large dipole moment of 6.76 D, [39] while its $A^3\Delta$ state has a significantly smaller value, 2.85 D similar to MoC. In our previous paper on MoS,[40] we noted that electronic states that leave the 5s-like 3σ orbital unoccupied have by far the greatest dipole moments, in the range of 5-7 D. In contrast, occupation of the 3σ orbital by one electron reduces the dipole moment to value of 2.5-5 D and double occupation of this orbital reduces the dipole moment further, to 1.5-2.5 D. We find much the same result in the MoC molecule, with the states where the 3σ orbital is empty ($X^3\Sigma^-$, $a^1\Gamma$, and $d^1\Sigma^+$) having dipole moments near 6 D while the states where the 3σ orbital is singly-occupied ($A^3\Delta$, $b^5\Sigma^-$, $c^1\Delta$, and $e^5\Pi$) have dipoles in the range of 2-3D. Occupation of the more diffuse 3σ orbital, which has significant electron density on the opposite side of the molecule from the negatively charged carbon atom, is quite effective in cancelling out much of the dipole moment of the molecule.

VI. CONCLUSIONS

The formation of quadruple bonds in diatomic molecules including second row atoms is not very common. Here, it is found that five low-lying states of the MoC molecule i.e., $X^3\Sigma^-$, $A^3\Delta$, $a^1\Gamma$, $c^1\Delta$, and $d^1\Sigma^+$ form quadruple bonds, $\sigma^2\sigma^2\pi^2\pi^2$, while the $b^5\Sigma^-$ and $e^5\Pi$ that result from the atoms in their ground states forms $\sigma^1\pi^2\pi^2$ and $\sigma^2\pi^2\pi^1$ bonds, respectively. All states have been examined meticulously using multireference configuration interaction methods in conjunction with a series of basis sets. Relativistic scalar effects and spin orbit interaction have also been calculated. We also report an experimental measurement of the bond dissociation energy (BDE) of the MoC molecule by identifying the onset of predissociation in the vibronic quasicontinuum using resonant two-photon ionization (R2PI) spectroscopy. This shifts the previous value, obtained by Knudsen effusion mass spectrometry, higher by 0.19 eV and reduces its error limit by a factor of 50, providing the most accurately measured value for the MoC BDE.

The $X^3\Sigma^-$, $A^3\Delta$, $a^1\Gamma$ and $d^1\Sigma^+$ states present avoided crossings. The $X^3\Sigma^-$ state dissociates to Mo (5S_g) + C (3P_g), but there is an avoided curve crossing at about 3.5 Å and the *in situ* atomic states that form the molecular ground state are Mo⁺(6S_g) + C⁻ (4S_u) or Mo(7S_g) + C(5S_u) with formation of a strongly polarized $1\sigma^2$ bond. The dissociation energy of the $X^3\Sigma^-$, $A^3\Delta$, $a^1\Gamma$, $c^1\Delta$, and $d^1\Sigma^+$ states, which

present a $\sigma^2\sigma^2\pi^2\pi^2$ bond, with respect to their adiabatic products are 6.472, 6.224, 7.231, 7.000, and 6.942 eV at the C-icMRCISD(+Q)/AWCV5Z(PP) level of theory. These states also have very similar bond distances ranging from 1.664 to 1.677 Å. Their large dissociation energies are a consequence of the quadruple bonding of the states. On the contrary, the $b^5\Sigma^-$ ($\sigma^1\pi^2\pi^2$) and $d^5\Pi$ ($\sigma^2\pi^2\pi^1$) states that correlate to the atomic ground state products, Mo (7S_g) + C (3P_g), have dissociation energies of 4.121 eV and 3.671 eV and bond lengths of 1.739 Å and 1.807 Å, respectively.

Spin-orbit coupling calculations have been performed for the first time. The $A_{\infty}^3\Delta_2$ electronic state is found to lie at 3899 cm^{-1} while the $c_{\infty}^1\Delta_2$ electronic state is at 8057 cm^{-1} , in very good agreement with the experimental values of DaBell *et al.* [9], 4002.5 and 7834 cm^{-1} , respectively. The $1_{\infty}^3\Delta_1$ and $1_{\infty}^3\Delta_3$ states are calculated to lie at 3334 and 4398 cm^{-1} , respectively.

Finally, the complete basis set limit of the calculated dissociation energy with respect to the atomic ground state products, Mo(7S_g) + C(3P_g), including corrections for scalar relativistic effects, is $D_e(D_0) = 5.13(5.06)$ eV; in excellent agreement with our D_0 experimental value of 5.136(5) eV. Furthermore, the calculated dissociation energy, D_e , at the CBS limit with respect to the adiabatic products, Mo(5S_g) + C(3P_g), is 6.61 eV, while with respect to the ionic products, $\text{Mo}^+(\text{}^6S_g) + \text{C}^-(\text{}^5S_u)$ is 10.92 eV. The calculated bond distance (r_e) is 1.670 Å, in good agreement with the value of $r_0 = 1.6760$ Å reported by Brugh *et al.*[7] via rotationally resolved spectroscopy.

SUPPLEMENTARY MATERIAL

The supplementary material provides absolute minimum energies for the $X^3\Sigma^-$, $A^3\Delta$, $a^1\Gamma$, $b^5\Sigma^-$, $c^1\Delta$, and $d^5\Pi$ states of MoC along with depictions of the MOs of the $X^3\Sigma^-$ ground state at internuclear separations of 3.5 and 4.0 Å. Also included is an Excel file that provides the spectra displayed in Figure 1.

ACKNOWLEDGMENTS

M.D.M. thanks the National Science Foundation for support of this research under Grant No. CHE-2305293.

AUTHOR DECLARATIONS

Conflict of Interest

The authors have no conflicts to disclose.

Author Contributions

Alexandros Androutsopoulos: Data curation (lead); Formal analysis (equal); Investigation (lead); Visualization (lead); Writing – original draft (lead). **Demeter Tzeli:** Conceptualization (lead); Data curation (equal); Formal analysis (lead); Investigation (lead); Methodology (lead); Project administration (lead); Resources (lead); Supervision (lead); Visualization (lead); Validation (lead); Writing – original draft (lead); Writing – review & editing (lead). **Kimberly H. Tomchak:** Conceptualization (equal); Data curation (lead); Investigation (lead); Methodology (equal); Writing – original draft (lead). **Michael D. Morse:** Conceptualization (lead); Data curation (equal); Funding acquisition (lead); Investigation (lead); Methodology (lead); Project administration (lead); Resources (lead); Supervision (lead); Validation (lead); Writing original draft (lead); Writing – review & editing (lead).

DATA AVAILABILITY

The data that support the findings of this study are available within the article and its Supporting Information. Further information may be obtained from the authors if needed.

REFERENCES

1. J. F. Harrison, "Electronic structure of diatomic molecules composed of a first-row transition metal and main-group element (H-F)," *Chem. Rev.* **100**, 679-716 (2000).
2. D. Tzeli and A. Mavridis, "Electronic structure and bonding of the 3d-transition metal borides, MB, M = Sc, Ti, V, Cr, Mn, Fe, Co, Ni, and Cu through all electron ab initio calculations," *J. Chem. Phys.* **128** 034309 (2008)
3. G. Schwarz, R. Mendel, M. Ribbe, "Molybdenum cofactors, enzymes and pathways," *Nature* **460**, 839–847 (2009).
4. Y. Deng, Y. Ge, M. Xu, Q. Yu, D. Xiao, S. Yao, D. Ma, "Molybdenum Carbide: Controlling the Geometric and Electronic Structure of Noble Metals for the Activation of O–H and C–H Bonds," *Acc. Chem. Res.* **52**, 3372-3383 (2019).
5. S. K. Gupta, K. A. Gingerich, "Mass spectrometric study of the stabilities of gaseous carbides of vanadium, niobium, and molybdenum," *J. Chem. Phys.* **74**, 3584-3590 (1981).
6. I. Shim, K. A. Gingerich, "Electronic states and nature of bonding in the molecule MoC by all electron ab initio calculations," *J. Chem. Phys.* **106**, 8093-8100 (1997).
7. D. J. Brugh, T. J. Ronningen, M.D. Morse, "First spectroscopic investigation of the 4d transition metal monocarbide MoC," *J. Chem. Phys.* **109**, 7851-7862 (1998).
8. X. Li, S. Liu, W. Chen, and L. S. Wang, "The electronic structure of MoC and WC by anion photoelectron spectroscopy," *J. Chem. Phys.* **111**, 2462-2469 (1999).

9. R. S. DaBell, R. G. Meyer, and M. D. Morse, "Electronic structure of the 4d transition metal carbides: Dispersed fluorescence spectroscopy of MoC, RuC, and PdC," *J. Chem. Phys.* **114**, 2938-54 (2001).
10. P. A. Denis and K. Balasubramanian, "Electronic states and potential energy curves of molybdenum carbide and its ions," *J. Chem. Phys.* **125**, 024306 (2006).
11. F. Stevens, I. Carmichael, F. Callens and M. Waroquier, "Density functional investigation of high-spin XY (X = Cr, Mo, W and Y = C, N, O) molecules," *J. Phys. Chem. A* **110**, 4846-53 (2006).
12. H. Wang, W. L. Virgo, J. Chen and T. C. Steimle, "Permanent electric dipole moment of molybdenum carbide," *J. Chem. Phys.* **127**, 124302/1-124302/6 (2007).
13. Q.-Y. Liu, L. Hu, Z.-Y. Li, C.-G. Ning, J.-B. Ma, H. Chen, S.-G. He, "Photoelectron imaging spectroscopy of MoC(-) and NbN(-) diatomic anions: A comparative study," *J. Chem. Phys.* **142**, 164301 (2015).
14. D. Tzeli and I. N. Karapetsas, "Quadruple Bonding in the Ground and Low-Lying Excited States of the Diatomic Molecules TcN, RuC, RhB, and PdBe," *J. Phys. Chem. A* **124**, 6667-6681 (2020)
15. D. Tzeli, "Quadruple chemical bonding in the diatomic anions TcN⁻, RuC⁻, RhB⁻, and PdBe⁻," *J. Comput. Chem.* **42**, 1126-1137 (2021)
16. K. A. Peterson, D. Figgen, M. Dolg, and H. Stoll, "Energy-consistent relativistic pseudopotentials and correlation consistent basis sets for the 4d elements Y-Pd," *J. Chem. Phys.* **126**, 124101 (2007); K. A. Peterson, T. H. Dunning, "Accurate correlation consistent basis sets for molecular core-valence correlation effects: The second row atoms Al-Ar, and the first row atoms B-Ne revisited," *J. Chem. Phys.* **117**, 10548-10560 (2002).
17. B. P. Prascher, D. E. Woon, K. A. Peterson, T. H. Dunning Jr, A. K. Wilson, "Gaussian basis sets for use in correlated molecular calculations. VII. Valence, core-valence, and scalar relativistic basis sets for Li, Be, Na, and Mg," *Theor. Chem. Acc.* **128**, 69-82 (2011).
18. R. A. Kendall, T. H. Dunning, R. J. Harrison, "Electron affinities of the first-row atoms revisited. Systematic basis sets and wave functions," *J. Chem. Phys.* **96**, 6796-6806 (1992).
19. M. Douglas and N. M. Kroll, "Quantum electrodynamical corrections to the fine structure of helium," *Ann. Phys.* **82**, 89-115 (1974); B. A. Hess, "Applicability of the no-pair equation with free-particle projection operators to atomic and molecular structure calculations," *Phys. Rev. A* **32**, 756 (1985); G. Jansen and B. A. Hess, "Revision of the Douglas-Kroll transformation," *Phys. Rev. A* **39**, 6016 (1989).

This is the author's peer reviewed, accepted manuscript. However, the online version of record will be different from this version once it has been copyedited and typeset.
PLEASE CITE THIS ARTICLE AS DOI: 10.1063/1.5011422

20. H.-J. Werner and P. J. Knowles, "An efficient internally contracted multiconfiguration-reference configuration interaction method," *J. Chem. Phys.* **89**, 5803 (1988);
21. P. J. Knowles and H.-J. Werner, "An efficient method for the evaluation of coupling coefficients in configuration interaction calculations," *Chem. Phys. Lett.* **145**, 514-522 (1988).
22. S. R. Langhoff and E. R. Davidson, "Configuration interaction calculations on the nitrogen molecule," *Int. J. Quantum Chem.* **8**, 61-72 (1974).
23. P. J. Knowles, G. Knizia, F. R. Manby, M. Schütz, P. Celani, W. Györffy, D. Kats, T. Korona, R. Lindh *et al*, MOLPRO 2015.1 is a package of *ab initio* programs written by H.-J. Werner.
24. K. A. Peterson, D. E. Woon, T. H. Dunning, "Benchmark calculations with correlated molecular wave functions. IV. The classical barrier height of the $H+H_2 \rightarrow H_2+H$ reaction," *J. Chem. Phys.* **100**, 7410-7415 (1994).
25. D. Tzeli, A. Mavridis, S. S. Xantheas, "A first principles study of the acetylene-water interaction," *J. Chem. Phys.* **112**, 6178-6189 (2000).
26. B. Paizs, P. Salvador, A. G. Császár, M. Duran, S. Suhai, "Intermolecular Bond Lengths: Extrapolation to the Basis Set Limit on Uncorrected and BSSE-Corrected Potential Energy Hypersurfaces," *J. Comput. Chem.*, **22**, 196–207 (2001).
27. D. Feller, "Benchmarks of improved complete basis set extrapolation schemes designed for standard CCSD(T) atomization energies," *J. Chem. Phys.* **138**, 074103 (2013).
28. E. L. Johnson, Q. C. Davis, M. D. Morse, "Predissociation measurements of bond dissociation energies: VC, VN, and VS," *J. Chem. Phys.* **144**, 234306 (2016).
29. D. J. Brugh, "Characterization of the Transition Metal Carbon Bond in Small Organometallic Molecules by Resonant Two-Photon Ionization Spectroscopy. Ph.D., University of Utah, Salt Lake City, Utah, (1997).
30. M. D. Morse, "Predissociation Measurements of Bond Dissociation Energies," *Acc. Chem. Res.* **52**, 119-126 (2019).
31. M. D. Morse, "Supersonic beam sources. In *Methods of Experimental Physics: Atomic, Molecular, and Optical Physics*, Dunning, F. B., Hulet, R. Eds.; Vol. II Atoms and Molecules; Academic Press, Inc., pp 21-47 (1996).
32. D. J. Matthew, M. D. Morse, "Resonant two-photon ionization spectroscopy of jet-cooled UN: Determination of the ground state," *J. Chem. Phys.* **138**, 184303 (2013).
33. W. C. Wiley and I. H. McLaren, "Time-of-Flight Mass Spectrometer with Improved Resolution," *Rev. Sci. Instrum.* **26**, 1150 - 1157 (1955).

This is the author's peer reviewed, accepted manuscript. However, the online version of record will be different from this version once it has been copyedited and typeset.
PLEASE CITE THIS ARTICLE AS DOI: 10.1063/5.0.11422

34. B. A. Mamyrin, V. I. Karataev, D. V. Shmikk and V. A. Zagulin, "Mass reflectron. New nonmagnetic time-of-flight high-resolution mass spectrometer," *Zh. Eksp. Teor. Fiz.* **64**, 82-9 (1973).
35. J. J. Sorensen, E. Tieu, A. Sevy, D. M. Merriles, C. Nielson, J. C. Ewigleben and M. D. Morse, "Bond dissociation energies of transition metal oxides: CrO, MoO, RuO, and RhO," *J. Chem. Phys.* **153**, 074303 (2020).
36. D. M. Merriles, K. H. Tomchak, J. C. Ewigleben and M. D. Morse, "Predissociation measurements of the bond dissociation energies of EuO, TmO, and YbO," *J. Chem. Phys.* **155**, 144303 (2021).
37. A. Kramida, Yu. Ralchenko, J. Reader, and NIST ASD Team (2023). NIST Atomic Spectra Database (version 5.11), <https://physics.nist.gov/asd> (National Institute of Standards and Technology Gaithersburg, MD (2023)).
38. D. Tzeli, A. Mavridis, "On the dipole moment of the ground state $X^3\Delta$ of iron carbide, FeC," *J. Chem. Phys.* **118**, 4984-4986 (2003).
39. A. Kalamos, T. H. Dunning, Jr., A. Mavridis, "First principles investigation of chromium carbide, CrC," *J. Chem. Phys.* **123**, 014302 (2005).
40. D. Tzeli, I. Karapetsas, D. M. Merriles, J. C. Ewigleben and M. D. Morse, "Molybdenum–Sulfur Bond: Electronic Structure of Low-Lying States of MoS," *J. Phys. Chem. A* **126**, 1168-1181 (2022).

Table 1. Previous theoretical and experimental data on the calculated states of MoC; bond length r_e (Å), dissociation energies D_e and D_0 (eV), vibrational frequency ω_e (cm^{-1}), anharmonic corrections $\omega_e x_e$ (cm^{-1}), dipole moment μ (Debye), and excitation energy T_e (cm^{-1}).

State	Methodology	r_e	D_e	D_0	ω_e	$\omega_e x_e$	μ	T_e
$X_{\square}^3\Sigma^-$	High temperature mass spectrometry ^a			4.95(0.17)				
	CASSCF/RC/[10s8p5d1f/Mo4s3p1d/c] ^b	1.693	5.199	5.139	971	1.69	6.15	
	MRCI/RC/[10s8p5d1f/Mo4s3p1d/c] ^b	1.688			997	1.69		
	R2PI spectroscopy ^c	1.6760						
	DF spectroscopy ^d				1008.3	3.3		
	MRCISD+Q/RECP/[5s3p3d1f/Mo3s3p1d/c] ^e	1.717	4.440		968		5.87	
	DFT/BP86/QZ4P ^f	1.667			1034.7		5.209	
	CCSD(T)/aug-cc-pwCVQZ(-PP) ^g	1.660						
	Anion photoelectron spectroscopy ^h				1000(100)			
High-resolution Stark spectroscopy ⁱ						6.07(0.18)		
$A_{\square}^3\Delta$	CASSCF/RC/[10s8p5d1f/Mo4s3p1d/c] ^b	1.692	5.81		1013		2.16	4500
	DF spectroscopy ($^3\Delta_2$ component) ^d				1003			4002.5
	MRCISD/RECP/[5s3p3d1f/Mo3s3p1d/c] ^e	1.711			998		2.77	3660
$a_{\square}^1\Gamma$	Anion photoelectron spectroscopy ^h							4120(200)
	CASSCF/RC/[10s8p5d1f/Mo4s3p1d/c] ^b	1.675			1042		6.14	7207
	MRCISD/RECP/[5s3p3d1f/Mo3s3p1d/c] ^e	1.693			1030		5.89	7647
$b_{\square}^5\Sigma^-$	Anion photoelectron spectroscopy ^h							5750(160)
	CASSCF/RC/[10s8p5d1f/Mo4s3p1d/c] ^b	1.769	2.80		891			6178
	MRCISD/RECP/[5s3p3d1f/Mo3s3p1d/c] ^e	1.779			873		2.46	5676
$c_{\square}^1\Delta$	Anion photoelectron spectroscopy ^h				[890(60)]			6290(80)
	CASSCF/RC/[10s8p5d1f/Mo4s3p1d/c] ^b	1.678	6.188		1026		1.44	9312
	DF spectroscopy ^d				1031			7834
$d_{\square}^1\Sigma^+$	MRCISD/RECP/[5s3p3d1f/Mo3s3p1d/c] ^e	1.697			1036		2.08	8198
	Anion photoelectron spectroscopy ^h				[890(60)]			7250(80)
	CASSCF/RC/[10s8p5d1f/Mo4s3p1d/c] ^b	1.676			1032			11639
$e_{\square}^5\Pi$	MRCISD/RECP/[5s3p3d1f/Mo3s3p1d/c] ^e	1.697			1022		5.83	9787
	CASSCF/RC/[10s8p5d1f/Mo4s3p1d/c] ^b	1.836	2.30		807			10228
	MRCISD/RECP/[5s3p3d1f/Mo3s3p1d/c] ^e	1.842			828		2.85	8740

^a Ref. 5. ^b Ref 6. ^c Ref. 7. ^d Ref. 9. ^e Ref. 10. ^f Ref. 11. ^g Ref.13. ^h Ref. 8. ⁱ Ref.12.

Table 2. Bond distances r_e (Å), adiabatic dissociation energies D_e (eV), harmonic frequencies ω_e (cm^{-1}), anharmonicities $\omega_e x_e$ (cm^{-1}), excitation energies T_e (cm^{-1}), and dipole moments μ (D) of the calculated states of MoC.

State	Basis Set	Method	r_e	D_e^a	D_e^b	D_0^b	ω_e	$\omega_e x_e$	T_e	$\langle \mu \rangle^c$	μ_{FF}^c
$X_{\text{e}}^3\Sigma^-$	A5ZPP	icMRCISD/	1.679	6.195	4.801	4.737	1027.5	7.21	0	6.00	5.96
		icMRCISD+Q	1.682	6.217	4.910	4.848	1022.2	7.29	0		5.92
	AWC5ZPP	C-icMRCISD	1.670	6.337	4.792	4.727	1042.9	6.76	0	5.99	5.88
		C-icMRCISD+Q^d	1.673	6.472	4.988	4.926	1038.3	6.76	0		5.83
	ATZDK	icMRCISD	1.686	6.068	4.662	4.598	1016.4	7.34	0	6.00	5.96
		icMRCISD+Q	1.689	6.077	4.757	4.692	1010.3	7.45	0		5.91
	AWCTZDK	C-icMRCISD	1.677	6.202	4.649	4.584	1034.7	7.22	0	5.98	5.87
		C-icMRCISD+Q	1.681	6.291	4.805	4.741	1028.3	7.30	0		5.81
$A_{\text{e}}^3\Delta$	A5ZPP	icMRCISD/	1.684	6.026	4.206	4.141	1030.9	6.83	4805	2.87	3.02
		icMRCISD+Q	1.686	5.986	4.368	4.304	1027.6	6.95	4373		3.05
	AWC5ZPP	C-icMRCISD	1.675	6.161	4.190	4.125	1038.9	7.08	4857	2.79	3.02
		C-icMRCISD+Q^d	1.677	6.224	4.504	4.440	1036.0	7.23	3900		3.12
	ATZDK	icMRCISD	1.689	5.874	4.106	4.042	1031.9	7.67	4485	2.89	3.01
		icMRCISD+Q	1.691	5.833	4.251	4.187	1027.5	7.83	4083		3.04
	AWCTZDK	C-icMRCISD	1.682	5.991	4.100	4.036	1032.0	6.84	4430	2.81	3.03
		C-icMRCISD+Q	1.685	6.006	4.363	4.299	1027.4	7.03	3565		3.11
$a_{\text{e}}^1\Gamma$	A5ZPP	icMRCISD/	1.668	7.114	3.972	3.905	1082	5.15	6689	5.92	5.86
		icMRCISD+Q	1.670	7.063	4.075	4.008	1077	5.25	6741		5.82
	AWC5ZPP	C-icMRCISD	1.662	7.218	4.032	3.965	1086	4.81	6079	5.94	5.82
		C-icMRCISD+Q^d	1.664	7.231	4.246	4.179	1081	4.98	5883		5.76
$b_{\text{e}}^5\Sigma^-$	A5ZPP	icMRCISD/	1.752	3.871	3.871	3.814	925	6.10	7455	2.32	2.55
		icMRCISD+Q	1.754	4.004	4.004	3.947	923	6.11	7323		2.60
	AWC5ZPP	C-icMRCISD	1.739	3.873	3.873	3.814	951	6.80	7243	2.16	2.52
		C-icMRCISD+Q^d	1.739	4.121	4.121	4.062	953	6.65	6886		2.63

$c\ ^1\Delta$	A5ZPP	icMRCISD/	1.674	6.849	3.662	3.597	1041.1	5.51	9194	2.48	2.36
		icMRCISD+Q	1.676	6.909	3.894	3.829	1040.3	5.59	8199		2.50
	AWC5ZPP	C-icMRCISD	1.665	6.829	3.586	3.520	1066.9	6.71	9728	2.43	2.29
		C-icMRCISD+Q^d	1.666	7.000	3.989	3.923	1065.5	6.78	8057		2.47
	ATZDK	icMRCISD	1.679	6.714	3.561	3.496	1043.8	6.56	8884	2.48	2.38
		icMRCISD+Q	1.681	6.754	3.772	3.707	1042.1	6.67	7943		2.51
	AWCTZDK	C-icMRCISD	1.672	6.712	3.503	3.437	1059.9	6.46	9242	2.44	2.30
		C-icMRCISD+Q	1.674	6.835	3.851	3.785	1057.2	6.60	7695		2.49
$d\ ^1\Sigma^+$	A5ZPP	icMRCISD/	1.672	6.785	-3.623	-3.686	1022.9	4.93	9507	5.92	5.94
		icMRCISD+Q	1.674	6.846	-3.922	-3.985	1017.1	5.01	7970		5.61
	AWC5ZPP	C-icMRCISD	1.663	6.757	-3.477	-3.541	1036.9	8.64	10559	5.93	6.04
		C-icMRCISD+Q^d	1.664	6.942	-3.915	-3.979	1030.1	8.92	8586		5.65
$e\ ^5\Pi$	A5ZPP	icMRCISD/	1.816	3.445	3.445	3.393	842	5.97	10941	2.89	3.12
		icMRCISD+Q	1.817	3.591	3.591	3.539	841	5.98	10639		3.18
	AWC5ZPP	C-icMRCISD	1.806	3.406	3.406	3.354	848	5.79	11128	2.75	3.11
		C-icMRCISD+Q^d	1.807	3.671	3.671	3.619	848	5.72	10548		3.22

^a Dissociation energies with respect to the correlated products. ^b Dissociation energies with respect to the ground state products.

^c $\langle\mu\rangle$ refers to expectation values and μ_{FF} to finite field values. ^d Our best calculated data in this Table are given in bold. Our final data at the CBS limit are given in Table 4, also in bold.

This is the author's peer reviewed, accepted manuscript. However, the online version of record will be different from this version once it has been copyedited and typeset.
PLEASE CITE THIS ARTICLE AS DOI: 10.1063/5.0211422

Table 3. Molecular orbitals including valence electrons in the minimum of the calculated states of the MoC molecule at C-icMRCISD/AWC5Z(PP).

State	Molecular Orbital	Main atomic orbitals
$X_{\square}^3\Sigma^-$	$1\sigma^2$	$0.88\varphi_{2s}(C) + 0.37\varphi_{4d_{z^2}}(Mo) + 0.20\varphi_{5s}(Mo) - 0.16\varphi_{2p_z}(C)$
	$2\sigma^2$	$0.68\varphi_{4d_{z^2}}(Mo) - 0.62\varphi_{2p_z}(C) - 0.22\varphi_{2s}(C)$
	$1\delta_+^1$	$1.00\varphi_{4d_{x^2-y^2}}(Mo)$
	$1\pi_x^2$	$0.64\varphi_{4d_{xz}}(Mo) + 0.59\varphi_{2p_x}(C)$
	$1\pi_y^2$	$0.64\varphi_{4d_{yz}}(Mo) + 0.59\varphi_{2p_y}(C)$
	$1\delta_-^1$	$1.00\varphi_{4d_{xy}}(Mo)$
$A_{\square}^3\Delta$	$1\sigma^2$	$0.92\varphi_{2s}(C) + 0.29\varphi_{5s}(Mo) + 0.26\varphi_{4d_{z^2}}(Mo) - 0.17\varphi_{4p_z}(Mo)$
	$2\sigma^2$	$0.82\varphi_{4d_{z^2}}(Mo) - 0.67\varphi_{2p_z}(C) + 0.21\varphi_{5s}(Mo)$
	$3\sigma^1$	$0.94\varphi_{5s}(Mo) - 0.17\varphi_{2p_z}(C) - 0.14\varphi_{2s}(C)$
	$1/\sqrt{2} 1\delta_+^1 + 1\delta_-^1\rangle$	$1/\sqrt{2} 1.00\varphi_{4d_{x^2-y^2}}(Mo) + 1.00\varphi_{4d_{xy}}(Mo)\rangle$
	$1\pi_x^2$	$0.74\varphi_{4d_{xz}}(Mo) + 0.56\varphi_{2p_x}(C)$
	$1\pi_y^2$	$0.74\varphi_{4d_{yz}}(Mo) + 0.56\varphi_{2p_y}(C)$
$a_{\square}^1\Gamma$	$1\sigma^2$	$0.89\varphi_{2s}(C) + 0.37\varphi_{4d_{z^2}}(Mo) - 0.22\varphi_{4p_z}(Mo) + 0.20\varphi_{5s}(Mo)$
	$2\sigma^2$	$-0.68\varphi_{4d_{z^2}}(Mo) + 0.62\varphi_{2p_z}(C) + 0.25\varphi_{6s}(C) + 0.21\varphi_{2s}(C)$
	$1\delta_+^1$	$0.99\varphi_{4d_{x^2-y^2}}(Mo)$
	π_x^2	$0.65\varphi_{4d_{xz}}(Mo) + 0.59\varphi_{2p_x}(C) - 0.11\varphi_{4p_x}(Mo)$
	π_y^2	$0.65\varphi_{4d_{yz}}(Mo) + 0.59\varphi_{2p_y}(C) - 0.11\varphi_{4p_y}(Mo)$
	$1\delta_-^1$	$0.99\varphi_{4d_{xy}}(Mo)$
$b_{\square}^5\Sigma^-$	$1\sigma^2$	$0.90\varphi_{2s}(C) + 0.28\varphi_{4d_{z^2}}(Mo) - 0.28\varphi_{4p_z}(Mo) + 0.15\varphi_{5s}(Mo)$
	$2\sigma^1$	$0.74\varphi_{2p_z}(C) - 0.47\varphi_{4d_{z^2}}(Mo) - 0.47\varphi_{5s}(Mo) + 0.31\varphi_{2s}(C)$
	$3\sigma^1$	$0.78\varphi_{5s}(Mo) - 0.51\varphi_{4d_{z^2}}(Mo) - 0.19\varphi_{5p_z}(Mo) + 0.11\varphi_{2p_z}(C)$
	$1\delta_+^1$	$0.99\varphi_{4d_{x^2-y^2}}(Mo)$
	π_x^2	$0.63\varphi_{4d_{xz}}(Mo) + 0.62\varphi_{2p_x}(C) - 0.10\varphi_{4p_x}(Mo)$
	π_y^2	$0.63\varphi_{4d_{yz}}(Mo) + 0.62\varphi_{2p_y}(C) - 0.10\varphi_{4p_y}(Mo)$
$1\delta_-^1$	$0.99\varphi_{4d_{xy}}(Mo)$	
$c_{\square}^1\Delta$	$1\sigma^2$	$0.92\varphi_{2s}(C) + 0.34\varphi_{5s}(Mo) + 0.32\varphi_{4d_{z^2}}(Mo) - 0.17\varphi_{4p_z}(Mo)$
	$2\sigma^2$	$-0.82\varphi_{4d_{z^2}}(Mo) + 0.63\varphi_{2p_z}(C) + 0.16\varphi_{5p_z}(Mo)$
	$3\sigma^1$	$0.89\varphi_{5s}(Mo) - 0.42\varphi_{5p_z}(Mo) - 0.26\varphi_{2p_z}(C)$
	$1/\sqrt{2} 1\delta_+^1 + 1\delta_-^1\rangle$	$1/\sqrt{2} 1.00\varphi_{4d_{x^2-y^2}}(Mo) + 1.00\varphi_{4d_{xy}}(Mo)\rangle$
	$1\pi_x^2$	$0.73\varphi_{4d_{xz}}(Mo) + 0.58\varphi_{2p_x}(C)$
	$1\pi_y^2$	$0.73\varphi_{4d_{yz}}(Mo) + 0.58\varphi_{2p_y}(C)$

This is the author's peer reviewed, accepted manuscript. However, the online version of record will be different from this version once it has been copyedited and typeset.
PLEASE CITE THIS ARTICLE AS DOI: 10.1063/5.0211422

$d_{\square}^1\Sigma^+$	$1\sigma^2$	$0.89\varphi_{2s(C)} + 0.19\varphi_{5s(Mo)} + 0.36\varphi_{4d_{z^2}(Mo)} - 0.22\varphi_{4p_z(Mo)}$
	$2\sigma^2$	$0.69\varphi_{4d_{z^2}(Mo)} - 0.62\varphi_{2p_z(C)} - 0.25\varphi_{5p_z(Mo)}$
	$1/\sqrt{2} 1\delta_+^2 + 1\delta_-^2\rangle$	$1/\sqrt{2} 1.00\varphi_{4d_{x^2-y^2}(Mo)} + 1.00\varphi_{4d_{xy}(Mo)}\rangle$
	$1\pi_x^2$	$0.65\varphi_{4d_{xz}(Mo)} + 0.59\varphi_{2p_x(C)}$
	$1\pi_y^2$	$0.65\varphi_{4d_{yz}(Mo)} + 0.59\varphi_{2p_y(C)}$
$e_{\square}^5\Pi$	$1\sigma^2$	$0.94\varphi_{2s(C)} - 0.20\varphi_{4p_z(Mo)} + 0.17\varphi_{4d_{z^2}(Mo)}$
	$2\sigma^2$	$0.71\varphi_{2p_z(C)} - 0.66\varphi_{4d_{z^2}(Mo)} + 0.21\varphi_{6s(C)} - 0.19\varphi_{5s(Mo)}$
	$3\sigma^1$	$0.91\varphi_{5s(Mo)} - 0.33\varphi_{4d_{z^2}(Mo)} - 0.18\varphi_{5p_z(Mo)}$
	$1\delta_+^1$	$0.99\varphi_{4d_{x^2-y^2}(Mo)}$
	π_x^1	$0.65\varphi_{4d_{xz}(Mo)} + 0.59\varphi_{2p_x(C)}$
	π_y^1	$0.65\varphi_{4d_{yz}(Mo)} + 0.59\varphi_{2p_y(C)}$
	$1\delta_-^1$	$0.99\varphi_{4d_{xy}(Mo)}$

This is the author's peer reviewed, accepted manuscript. However, the online version of record will be different from this version once it has been copyedited and typeset.
PLEASE CITE THIS ARTICLE AS DOI: 10.1063/5.0211422

Table 4. Bond distances r_e (Å), dissociation energies D_e and D_0 (eV) with respect to the ground state atomic products, harmonic frequencies ω_e (cm^{-1}) of the ground state, $X_{\text{e}}^3\Sigma^-$, of MoC at the C-icMRCISD and C-icMRCISD+Q/aug-cc-pwCVnZ(-PP), $n = \text{D}(2), \text{T}(3), \text{Q}(4)$, and 5 levels of theory and the corresponding CBS limits with different approaches.

	r_e	D_e	D_0	ω_e	r_e	D_e	D_0	ω_e
	C-icMRCISD				C-icMRCISD+Q			
AWCDZ(PP)	1.701	4.144	4.081	1015	1.706	4.254	4.192	1007
AWCTZ(PP)	1.677	4.572	4.508	1024	1.680	4.753	4.690	1019
AWCQZ(PP)	1.672	4.719	4.655	1032	1.674	4.921	4.857	1028
AWC5Z(PP)	1.669	4.791	4.726	1043	1.672	4.988	4.923	1038
CBS [I; 1]^a	1.667	4.833	4.768		1.671	5.027	4.961	
CBS [II; 1]^a	1.667	4.834	4.770		1.671	5.027	4.963	
CBS [I; 2]^a	1.666	4.938	4.866		1.670	5.075	5.007	
CBS [II; 2]^a	1.666	4.913	4.849		1.670	5.073	5.009	
AWCTZDK	1.677	4.649	4.584	1035	1.681	4.805	4.741	1028.3
Diff^b	0.001	0.077	0.076		0.001	0.052	0.051	
CBS^c	1.667	5.02	4.94		1.671	5.13	5.06	
Expt					1.6760 ^d		4.95±0.17 ^e	
Expt							5.136±0.003 ^f	

^a 1: Mixed Gaussian/exponential form (1); 2: Power function extrapolation scheme (2); I: approach I, II: approach II (computational details); r_e : error bars $<\pm 0.001$ Å; D_e or D_0 : error bars $<\pm 0.01$ eV.

^b Correlation energy difference between C-icMRCISD(+Q)/aug-cc-pwCVTZ(-PP) and C-icMRCISD(+Q)/aug-cc-pwCVTZ-DK.

^c CBS limits including the correlation energy difference between DK and relativistic pseudopotential. Our best data given in bold.

^d r_0 value from Ref. 7. ^e Ref. 5. ^f Present study.